Biological pattern formation: beyond classical diffusion-based mechanisms

Paul C Bressloff

Department of Mathematics, University of Utah

October 19, 2021

Outline of talk

I. Cytoneme-based morphogenesis

II. Switching diffusions and protein gradients in the *C. elegans* zygote

III. Intracellular Turing pattern formation

Diffusion-based morphogen gradients[1]

- A spatially varying concentration of a morphogen protein drives a corresponding spatial variation in gene expression through a thresholding mechanism.
- Continuously varying morphogen concentration $\Longrightarrow$ discrete spatial pattern of differentiated gene expression across a cell population.
- Basic mechanism of morphogen gradient formation involves a localized source of protein production within the embryo, combined with diffusion away from the source and subsequent degradation.

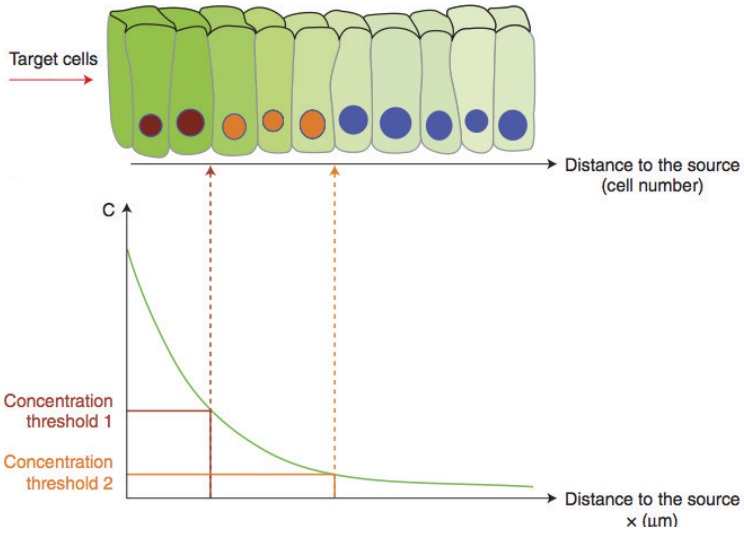

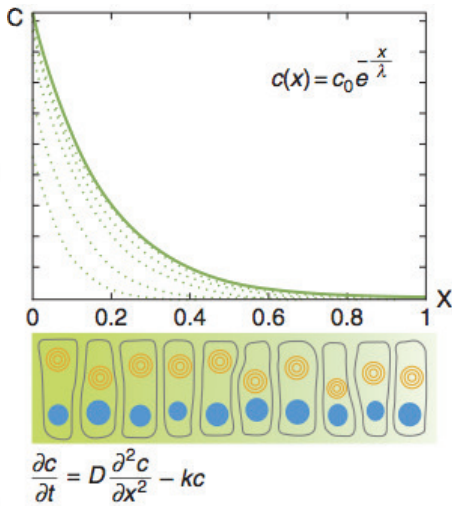

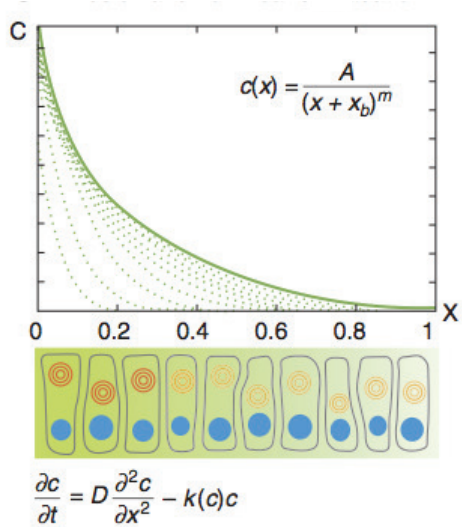

[1] L. Wolpert 1969

CYTONEME-BASED MORPHOGEN GRADIENTS[2]

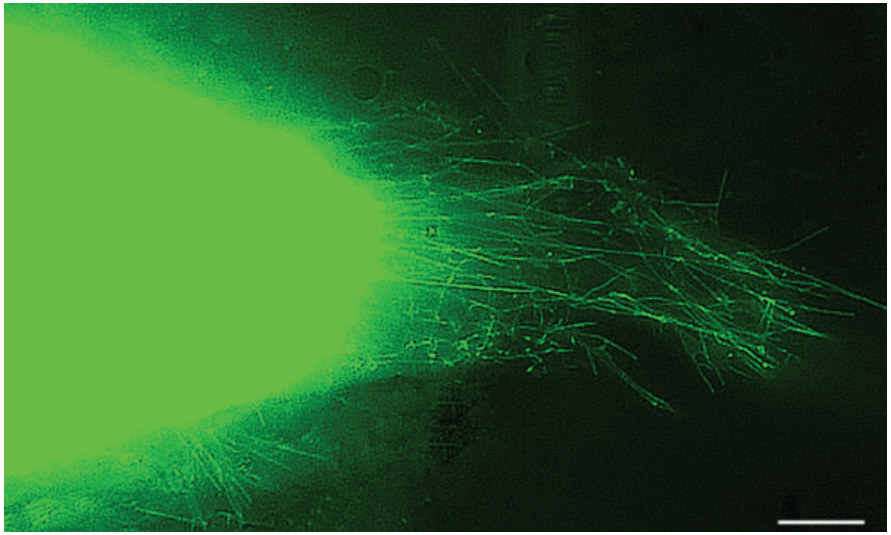

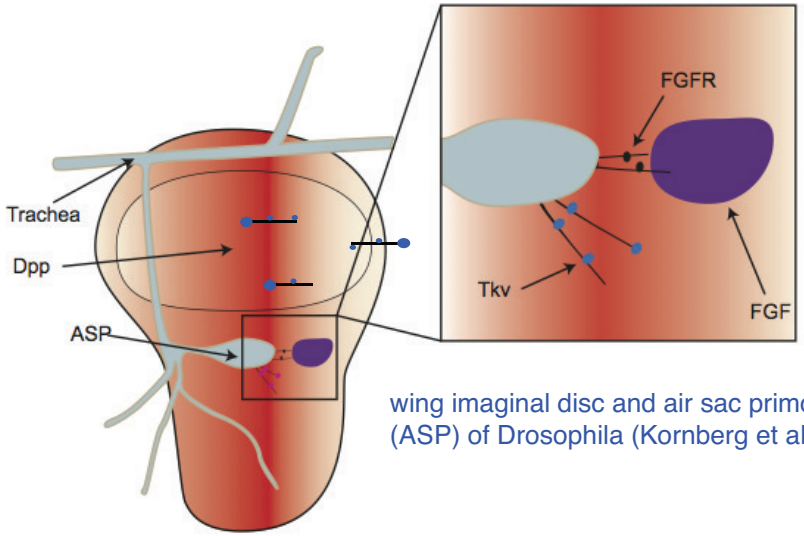

wing imaginal disc and air sac primordium (ASP) of Drosophila (Kornberg et al)

- Cytonemes are long, thin actin-rich protrusions varying in length from 1-200 μm. Allow for the active transport of morphogens or their cognate receptors between cells.
- They have been observed in many types of cells and in many developmental contexts, including the imaginal wing disc of Drosophila (Dpp and Hh), sonic hedgehog (Shh) cell-to-cell signaling in chicken limb buds, and Wnt signaling in zebrafish.

[2] T. Kornberg 2014

Filopodia play a role in within-host spread of Covid-19[3]

- Infection promotes host MAPK cascade activity and shutdown of mitotic kinases
- Infection stimulates filopodial protrusions with budding virus

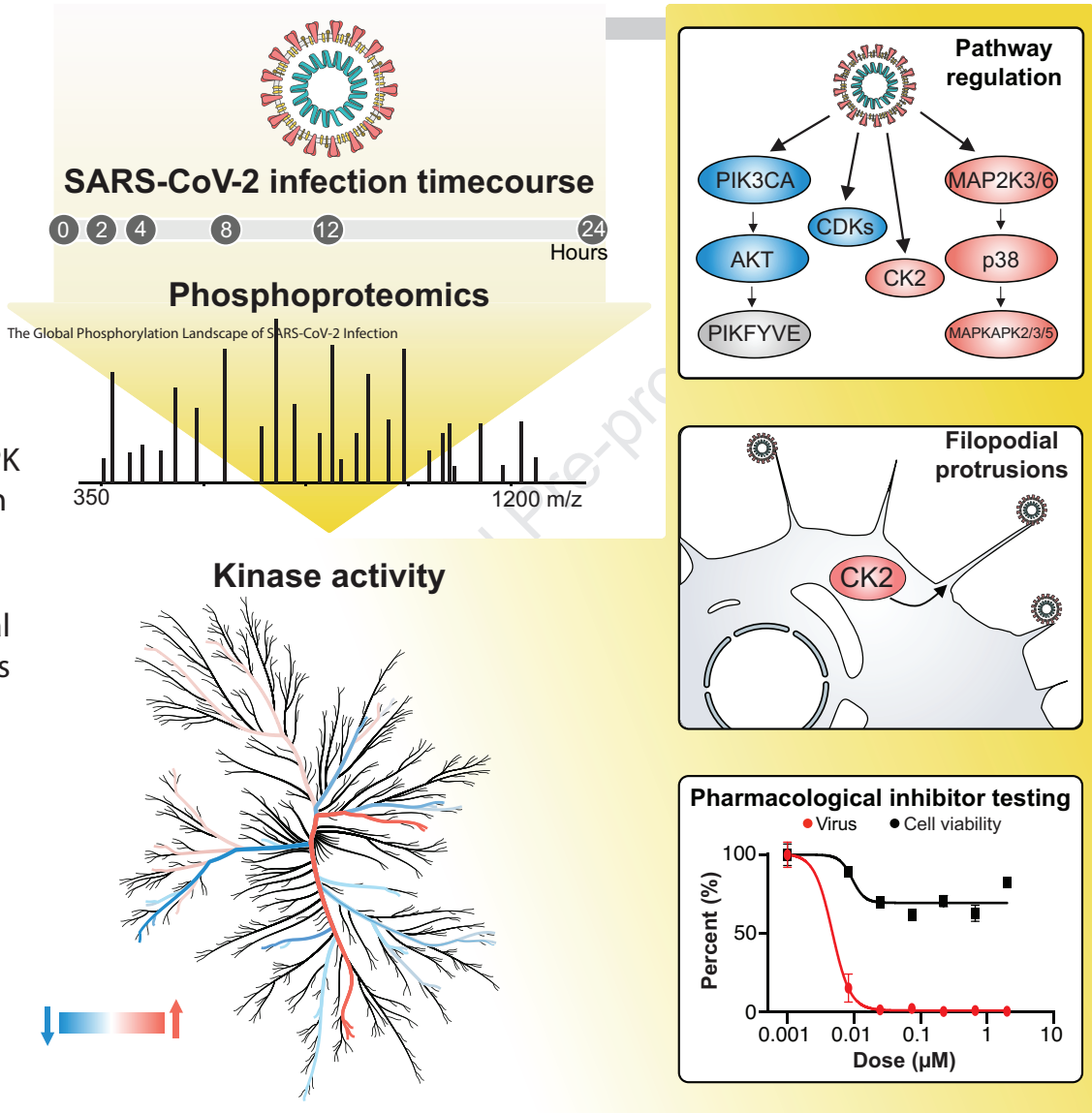

[3] Bouhaddu et al Cell 182 (3) 2020

Cytoneme-based morphogenesis

Drosophila wing disc and Shh signaling in chicks

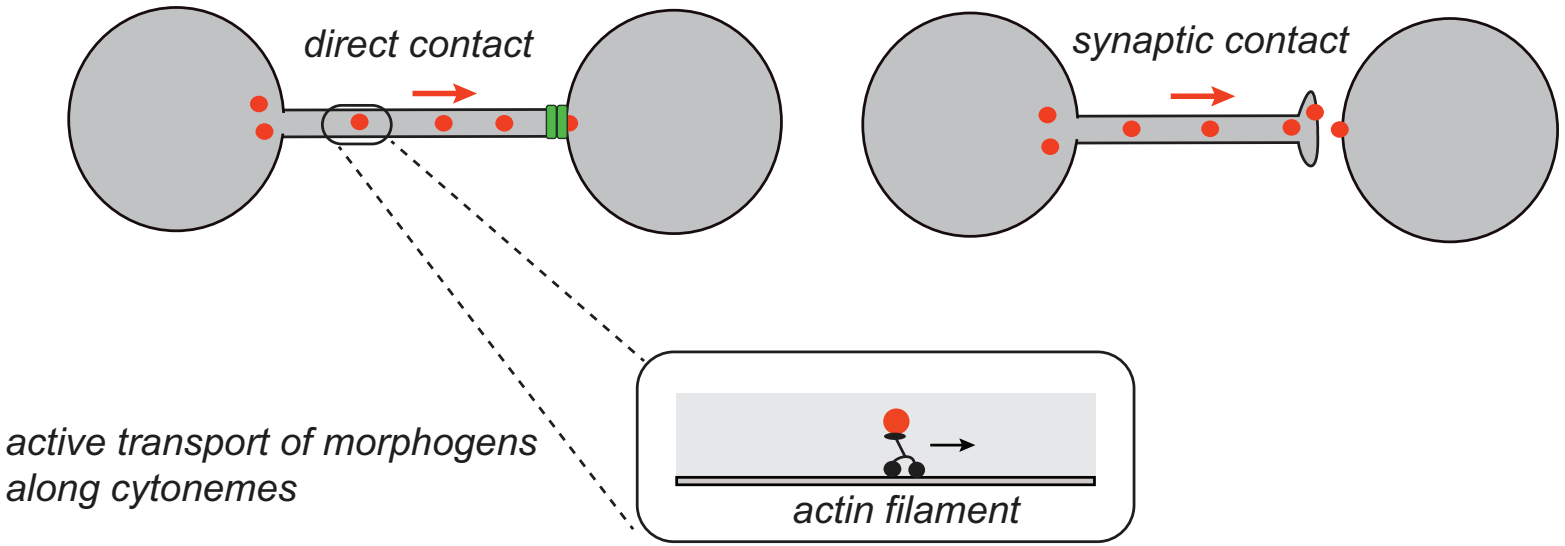

Wnt signaling in zebrafish

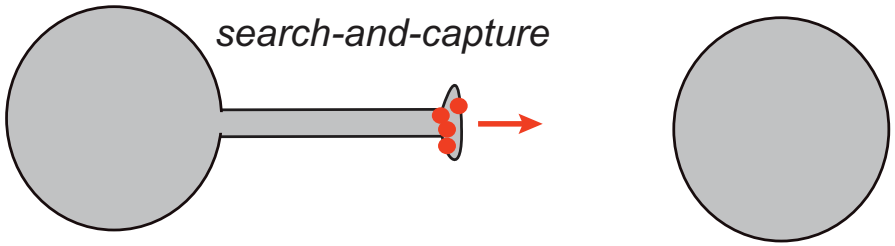

morphogens located at the tip of a growing cytoneme

DIRECTED SEARCH-AND-CAPTURE MODEL OF CYTONEMES[4]

- Single cytoneme nucleates in a random direction from a source cell. Probability of orientation to kth target cell is p_k with $\sum_k p_k < 1$.
- One end of the cytoneme is fixed at $x = 0$, and the position of the other end is taken to be a stochastic variable $X(t)$ (length of the cytoneme).
- Filament randomly switches from a growing state with tip speed v_+ to retraction phase with tip speed v_-. Switching times distributed exponentially with rate r.

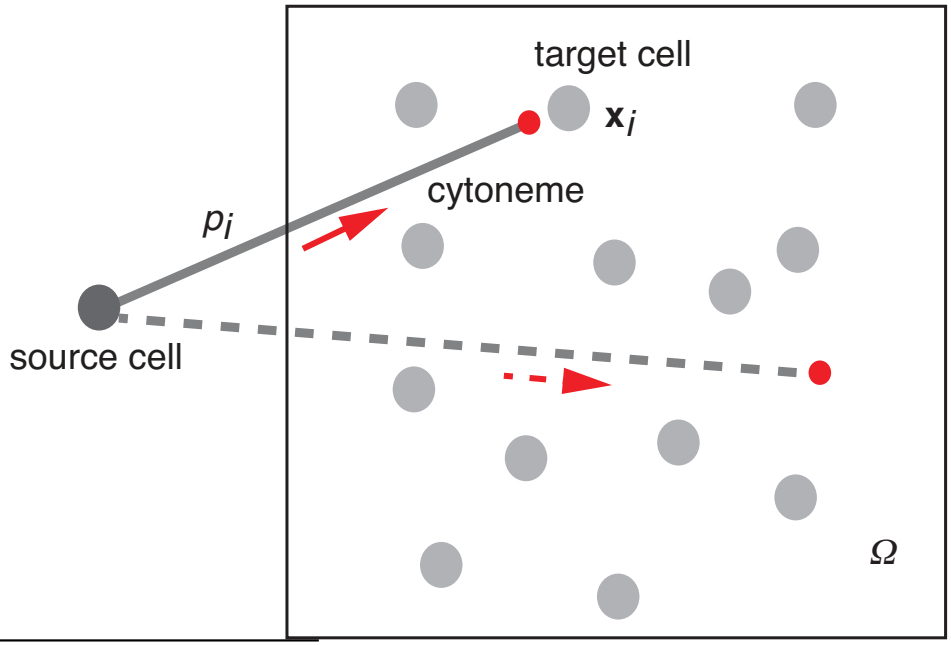

[4] PCB and Kim 2019,PCB 2020

SINGLE TARGET

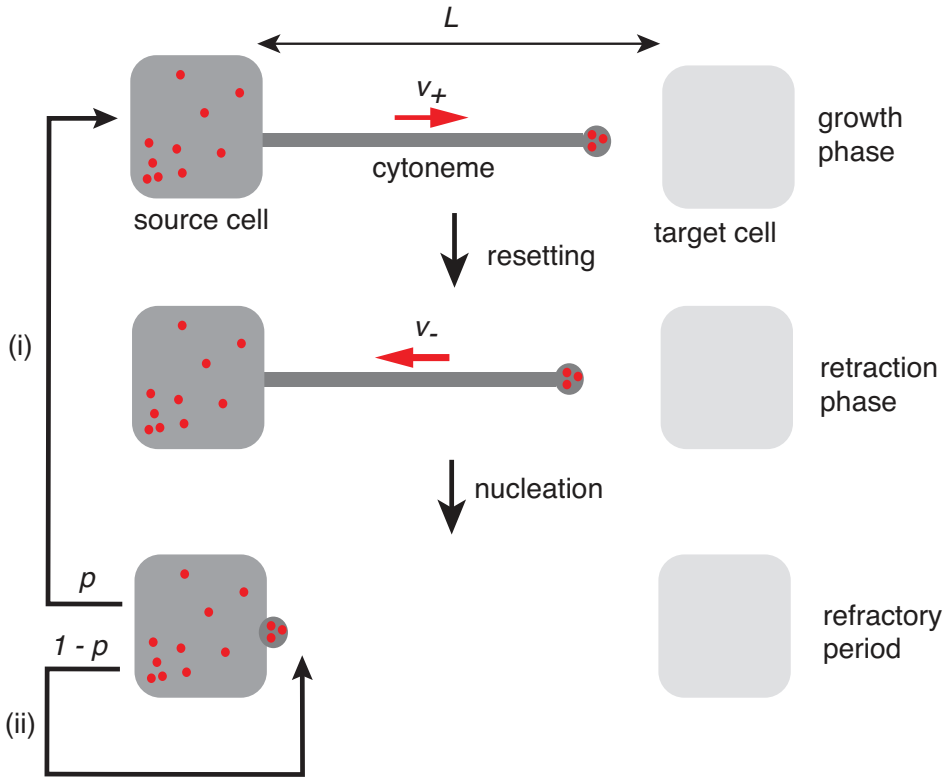

- Chapman-Kolmogorov equation

$$\frac{\partial p_+}{\partial t} = -v_+ \frac{\partial p_+}{\partial x} - r p_+, \; x \in (0, L),$$
$$\frac{\partial p_-}{\partial t} = v_- \frac{\partial p_-}{\partial x} + r p_+,$$
$$\frac{dP_0}{dt} = v_- p_-(0,t) - \eta P_0(t),$$

with boundary conditions

$$v_+ p_+(0,t) = \eta P_0(t), \quad p_-(L,t) = 0.$$

and initial conditions

$$P_0(0) = 0, \quad p_n(x,0) = \delta_{n,+}\delta(x).$$

- resetting rate r, nucleation rate η

MEAN FIRST PASSAGE TIME (MFPT) FOR $p = 1$

- Given the boundary conditions one finds that

$$\frac{d}{dt}\int_0^L p(x,t)dx + \frac{dP_0}{dt} = -v_+ p_+(L,t) \equiv -J(t),$$

  where $J(t)$ is the probability flux into the target.
- Introduce the survival probability

$$Q(t) = \int_0^L p(x,t)dx + P_0(t),$$

- The first passage time density $f(t)$ is

$$f(t) = -\frac{dQ(t)}{dt} = J(t).$$

  and the MFPT T for the cytoneme to be captured by the target is

$$T = -\int_0^\infty t\frac{dQ(t)}{dt}dt = \int_0^\infty Q(t)dt.$$

RENEWAL METHOD

- Exploits the fact that resetting eliminates any memory of previous search stages.
- Consider the following set of first passage times;

$$\mathcal{T} = \inf\{t > 0; X(t) = L\}, \text{ FPT with an arbitrary number of resettings}$$
$$\mathcal{S} = \inf\{t > 0; X(t) = 0\}, \text{ FPT for the first resetting and return to the origin}$$
$$\mathcal{R} = \inf\{t > 0; X(t + \mathcal{S} + \tau) = L\}, \text{ FPT with at least one resetting.}$$

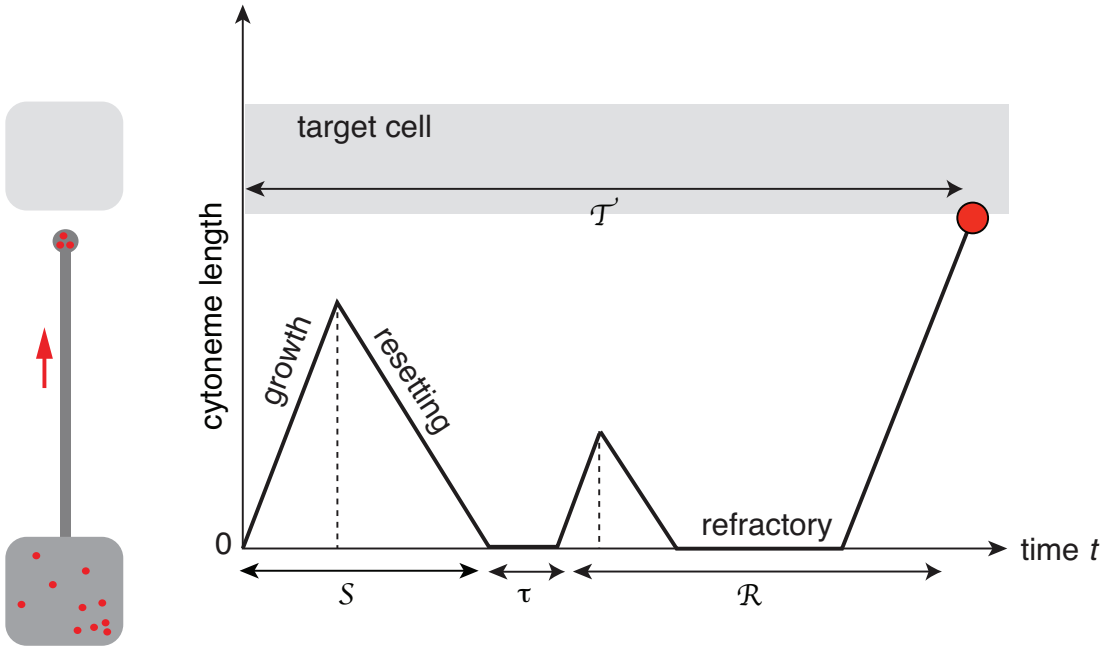

RENEWAL METHOD

- Let $\Omega = \{\mathcal{T} < \infty\}$ be the set of all events for which the particle is eventually absorbed by the target (which has measure one),
- Let $\Gamma = \{\mathcal{S} < \mathcal{T} < \infty\} \subset \Omega$ be the subset of events in Ω for which the particle resets at least once.
- It follows that $\Omega \backslash \Gamma = \{\mathcal{T} < \mathcal{S} = \infty\}$ is the set of all events for which the particle is captured by the target without any resetting.
- Introduce the decomposition

$$\mathbb{E}[\mathcal{T}] = \mathbb{E}[\mathcal{T} 1_{\Omega\backslash\Gamma}] + \mathbb{E}[\mathcal{T} 1_{\Gamma}].$$

- Probability of no resetting up to time t is $\Psi(t) = \mathrm{e}^{-rt}$ and the survival probability without resetting is $Q_0(t) = H(L/v_+ - t)$. Hence

$$\mathbb{E}[\mathcal{T} 1_{\Omega\backslash\Gamma}] = -\int_0^\infty t\mathrm{e}^{-rt} \frac{dQ_0(t)}{dt} dt = \left(1 + r\frac{d}{dr}\right) \widetilde{Q}_0(r),$$

where

$$\widetilde{Q}_0(r) = \frac{1}{r}\left(1 - \mathrm{e}^{-rL/v_+}\right).$$

RENEWAL METHOD

- The second expectation can be further decomposed as

$$\mathbb{E}[\mathcal{T}1_\Gamma] = \mathbb{E}[(\mathcal{S}+\tau+\mathcal{R})1_\Gamma] = \mathbb{E}[\mathcal{S}1_\Gamma] + (\overline{\tau}+T)\mathbb{P}[\Gamma].$$

  where $\mathbb{E}[\tau] = \overline{\tau}$ is the mean refractory (nucleation) period
- The result $\mathbb{E}[\mathcal{R}1_\Gamma] = TP[\Gamma]$ follows from the fact that return to the origin restarts the stochastic process without any memory.
- Calculation of $\mathbb{E}[\mathcal{S}1_\Gamma]$: first resetting occurs with probability $re^{-rt}Q_0(t)dt$ in the interval $[t, t+dt]$. At time t the particle is at position v_+t and thus takes an additional time v_+t/v_- to return to $x=0$. Hence

$$\mathbb{E}[\mathcal{S}1_\Gamma] = \int_0^\infty re^{-rt}t\left(1+\frac{v_+}{v_-}\right)Q_0(t)dt = -r\left(1+\frac{v_+}{v_-}\right)\frac{d}{dr}\widetilde{Q}_0(r).$$

- From the definitions of the first passage times and the effect of resetting,

$$\mathbb{P}[\Gamma] = \mathbb{P}[\mathcal{S}<\infty]\mathbb{P}[\mathcal{R}<\infty],$$

  with $\mathbb{P}[\mathcal{R}<\infty] = 1$ and

$$\mathbb{P}[\mathcal{S}<\infty] = \int_0^\infty re^{-rt}Q_0(t)dt = r\widetilde{Q}_0(r).$$

FINAL RESULT[5]

- Combining the various results yields an implicit equation for T:

$$T = \left(1 + r\frac{d}{dr}\right)\widetilde{Q}_0(r) + r\overline{\tau}\widetilde{Q}_0(r) - r\left(1 + \frac{v_+}{v_-}\right)\frac{d}{dr}\widetilde{Q}_0(r) + r\widetilde{Q}_0(r)T.$$

  Rearranging this equation yields the final result

$$T = \frac{\widetilde{Q}_0(r) + r\overline{\tau}\widetilde{Q}_0(r) - r\frac{v_+}{v_-}\widetilde{Q}_0'(r),}{1 - r\widetilde{Q}_0(r)}.$$

- This is a general formula for a dynamical process with stochastic resetting, finite return times and refractory periods. For our particular model,

$$T = T(L) := \frac{1}{r}\left[(\mathrm{e}^{rL/v_+} - 1)(1 + r\overline{\tau} + v_+/v_-) - \frac{rL}{v_-}\right].$$

  In the limit $r \to 0$, $T(L) \to L/v_+$, which is simply the deterministic time for the cytoneme tip to travel the distance L.

[5] PCB 2020

SEARCH WITH $p < 1$: OPTIMAL RESETTING RATES

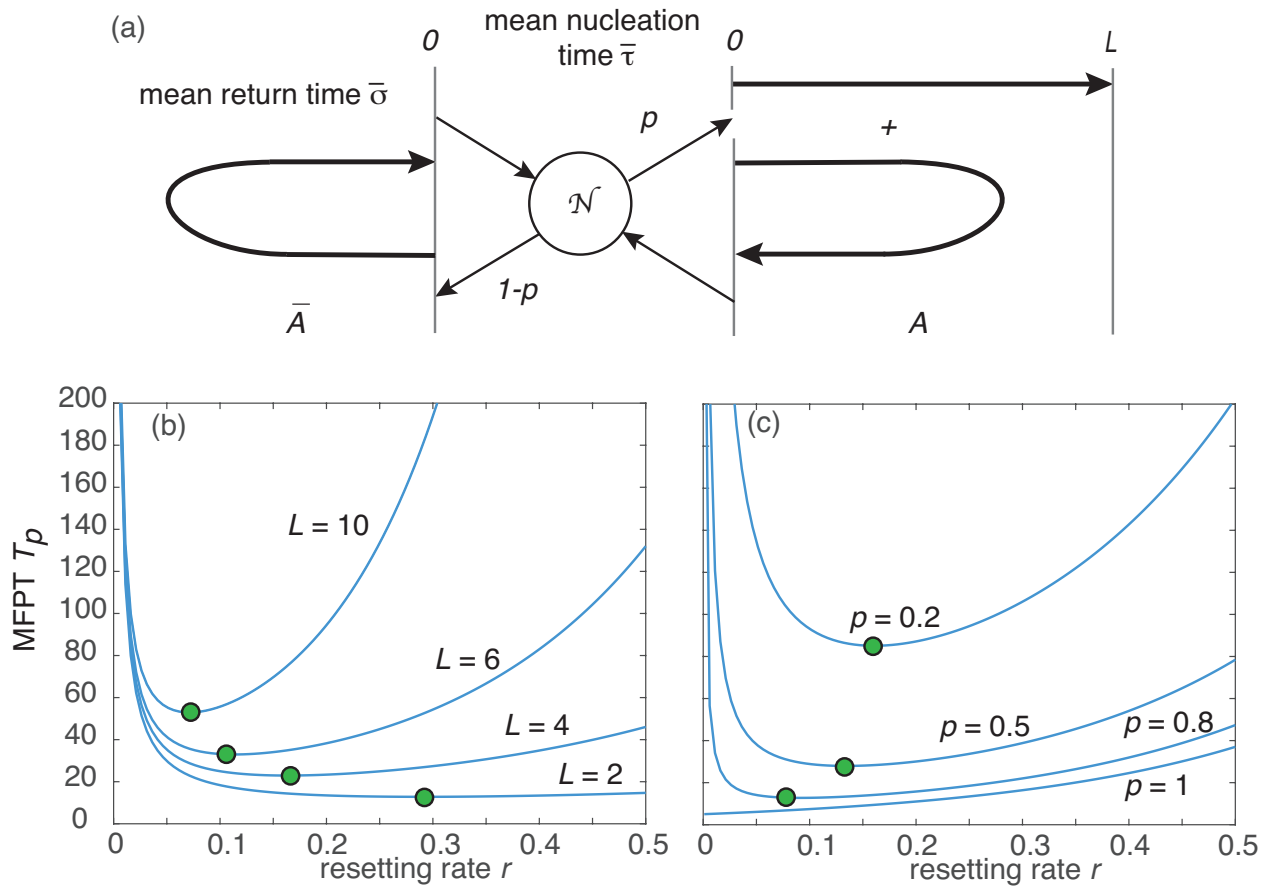

$$T_p = \frac{1}{1 - r\widetilde{Q}_0(r)} \left\{ \frac{(1-p)[\bar{\tau} + \bar{\sigma}]}{p} + \widetilde{Q}_0(r) + r\bar{\tau}\widetilde{Q}_0(r) - r\frac{v_+}{v_-}\widetilde{Q}_0'(r) \right\}.$$

MULTIPLE TARGETS

- Can extend the renewal method to multiple targets
- Introduce the FPT to find the j-th target:

$$\mathcal{T}_j = \inf\{t \geq 0; X(t) = L_j,\ I(t) \geq 0\}$$

  with $\mathcal{T}_j = \infty$ if another target is found.

- Introduce the set of events that particle finds j-th target: $\Omega_j = \{\mathcal{T}_j < \infty\}$
- The splitting probability that the cytoneme finds the j-th target is

$$\pi_j = \mathbb{E}[1_{\Omega_j}] = \mathbb{P}[\Omega_j] = \frac{p_j \mathrm{e}^{-rL_j/v_+}}{\sum_{l=1}^{N} p_l \mathrm{e}^{-rL_l/v_+}},$$

- Since MFPT to find a given target is infinite, we need to condition on the set of events Ω_j. Define conditional MFPT as

$$\pi_j T_j = \mathbb{E}[\mathcal{T}_j 1_{\Omega_j}].$$

MULTIPLE SEARCH-AND-CAPTURE EVENTS[6]

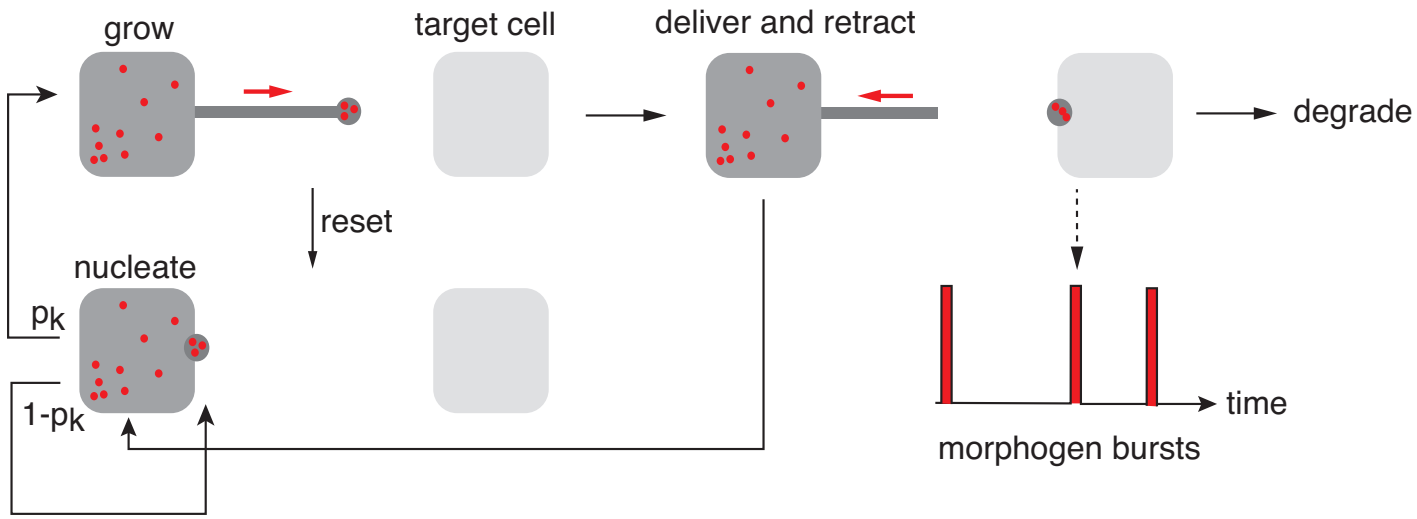

- Stages of a single search-and-capture process culminating in delivery of a burst of morphogen to the kth target cell.

  (i) Alternating periods of growth, shrinkage.

  (ii) Nucleation whenever the cytoneme shrinks to zero

  (iii) When a cytoneme is captured by a target cell, it delivers a morphogen burst and then retracts back to the nucleation site.

[6] PCB and Kim 2019, PCB 2020

MAPPING BETWEEN QUEUING THEORY AND MORPHOGEN BURSTING

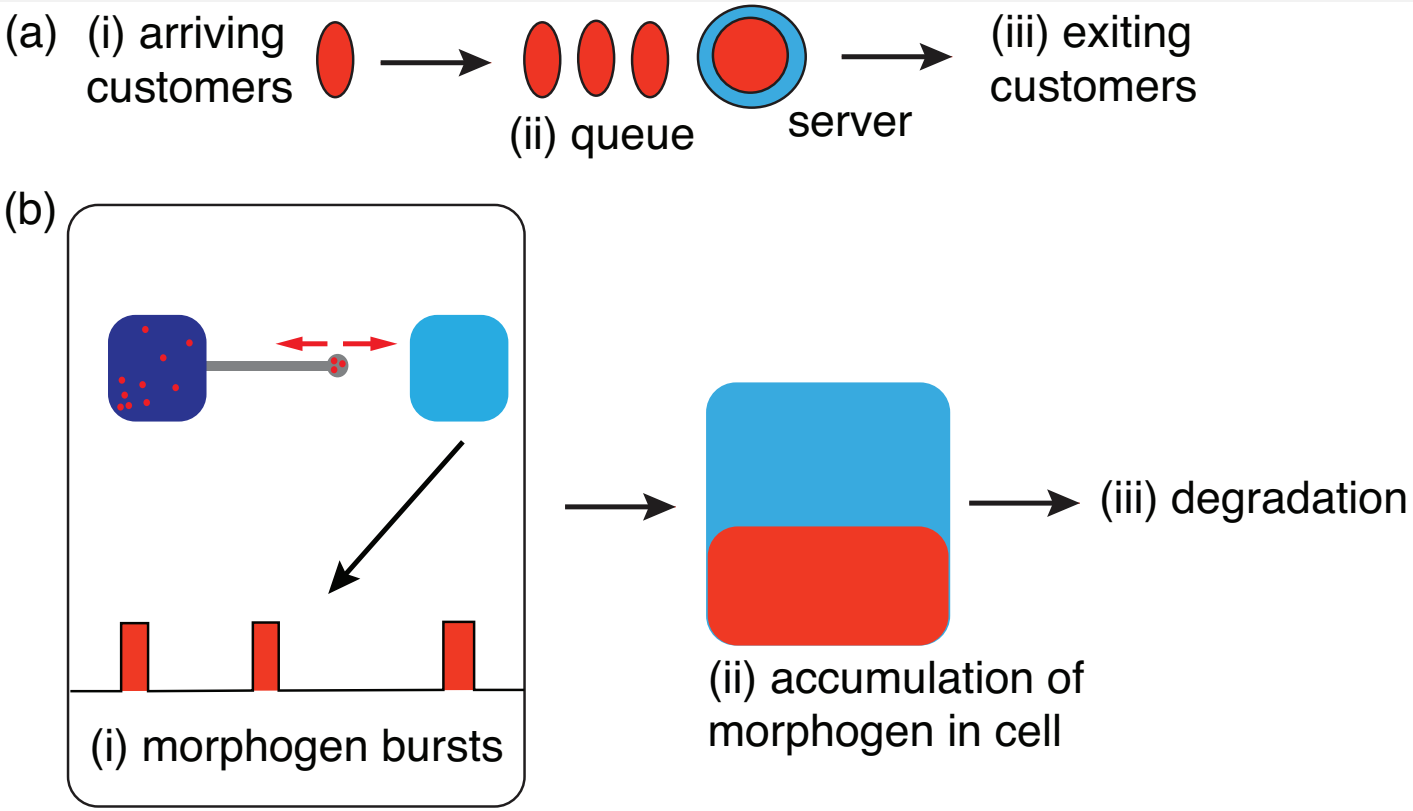

- Multiple search-and-capture events generates a sequence of morphogen bursts within a target cell - analogous to the arrival of customers in a queuing model.
- Accumulation of morphogen within the cell, is the analog of a queue.
- Independent particle degradation corresponds to exiting of customers after being serviced by an infinite number of servers

QUEUING MODEL $G/M/\infty$

- The particular queuing model is the $G/M/\infty$ system.
- Here the symbol G denotes a general inter-arrival time distribution
- The symbol M stands for a Markovian or exponential service-time distribution $H(t) = 1 - \mathrm{e}^{-\gamma t}$ for morphogen degradation at a rate γ, and '∞' denotes infinite servers.
- We can write for each inter-event time Δ and target $\mathcal{K}(\Delta)$

$$F_j(t) := \mathbb{P}[\Delta < t, \mathcal{K}(\Delta) = k] = \mathbb{P}[\Delta < t, |\mathcal{K}(\Delta) = k]\mathbb{P}[\mathcal{K}(\Delta) = k]$$
$$= \pi_j \int_0^t f_j(\tau) d\tau$$

- $f_j(\tau)$ is the conditional FPT density for a single search-and-capture event that terminates at the jth cell.

$$T_j = \int_0^\infty \tau f_j(\tau) d\tau$$

RESULTS: MULTIPLE SEARCH-AND-CAPTURE EVENTS

- Let M_k be the steady-state number of resource packets in the k-th target. The mean is (Little's law)

$$\overline{M}_k = \frac{\pi_k}{\gamma \sum_{j=1}^{N} \pi_j (T_j + \tau_{\text{cap}})} = \frac{\pi_k}{\gamma (T + \tau_{\text{cap}})},$$

  where $\tau_{\text{cap}} = \int_0^\infty \rho(\tau) d\tau$ is the mean loading/unloading time and $T = \sum_{j=1}^{N} \pi_j T_j$ is the unconditional MFPT
- $T + \tau_{\text{cap}}$ is the mean time for one successful delivery of a packet to any one of the targets and initiation of a new round of search-and-capture. Its inverse is the mean rate of capture events and π_k is the fraction that are delivered to the k-th target (over many trials).
- The k-dependence of $\overline{M}_k$ specifies the morphogen gradient
- The variance is

$$\text{Var}[M_k] = \overline{M}_k \left[\frac{\pi_k \widetilde{f}_k(\gamma)}{1 - \sum_{j=1}^{N} \pi_j \widetilde{f}_j(\gamma)} + 1 - \overline{M}_k \right].$$

EXAMPLE: SINGLE LAYER OF TARGET CELLS

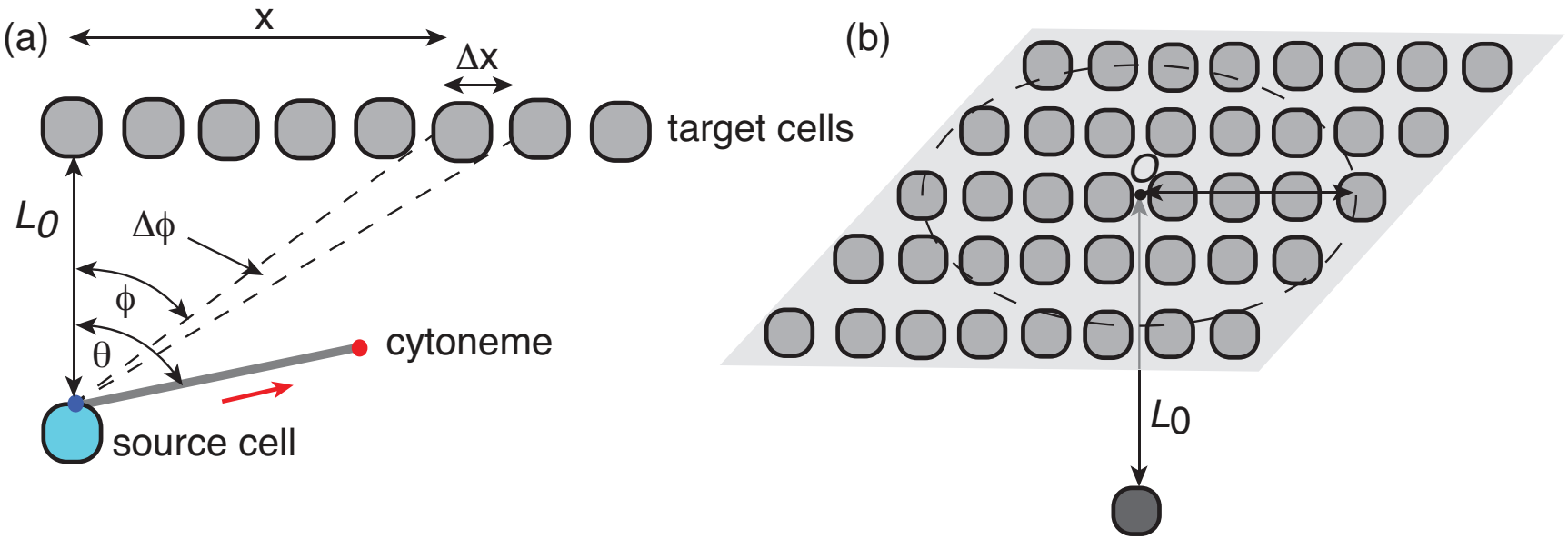

- Single 1D layer: Suppose that the k-th target cell subtends an angle $\Delta\phi_k$ and that the distribution of cytoneme directions is uniform on $[0, \pi/2]$.
- Moreover, $\Delta\phi_{k+1} \approx \phi(x_k + \Delta x) - \phi(x_k)$, where $\tan\phi(x) = x/L_0$, L_0 is the perpendicular distance of the source cell from the target layer, and $x_k = k\Delta x$.
- It follows that

$$p_{k+1} \approx \frac{2\Delta\phi_{k+1}}{\pi} = \frac{2}{\pi}\sec^{-2}(\phi_k)\frac{\Delta x}{L_0} = \left(1 + \frac{x_k^2}{L_0^2}\right)^{-1}\frac{\Delta x}{L_0}. = \frac{2\Delta x L_0}{\pi L_k^2}, \quad L_k^2 = L_0^2 + x_k^2$$

RESULTS AND EXTENSIONS

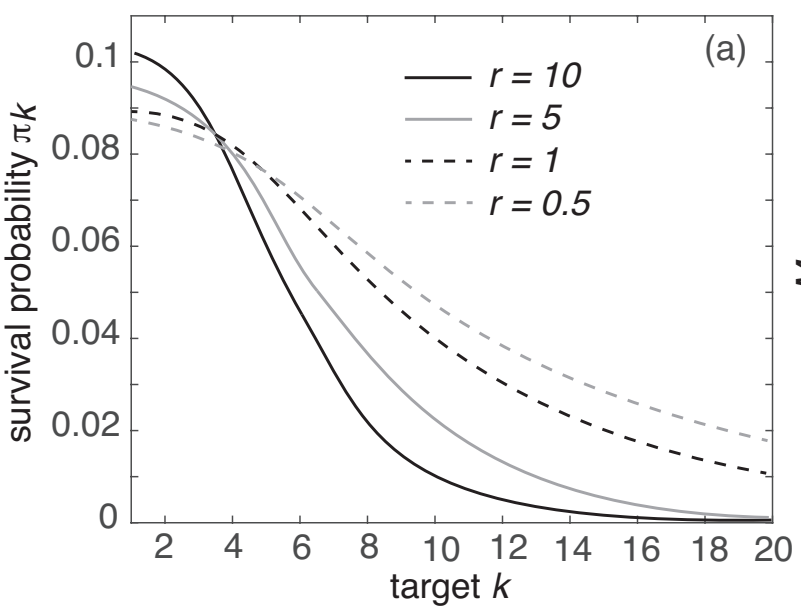

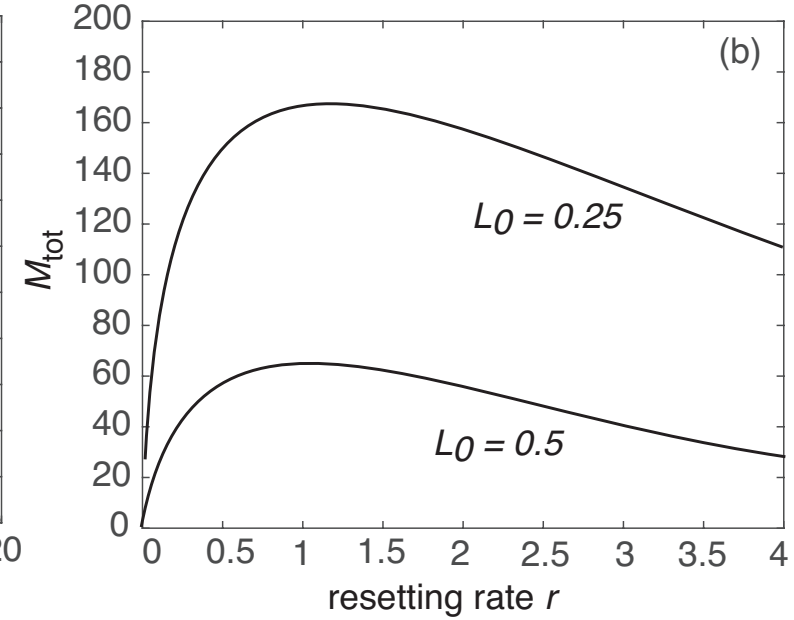

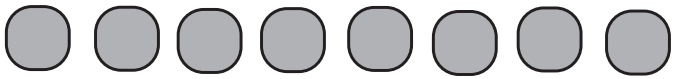

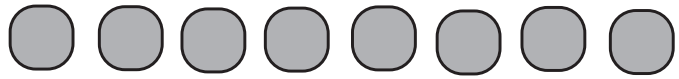

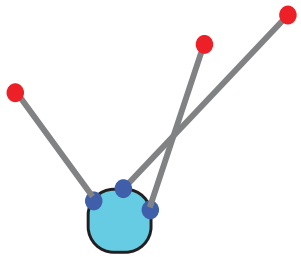

multiple nucleation sites

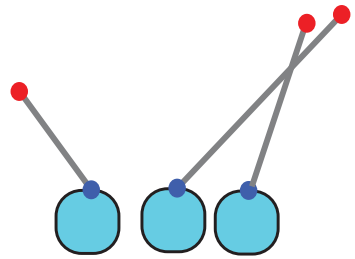

multiple source cells

Outline of talk

I. Cytoneme-based morphogenesis

II. Switching diffusions and protein gradients in *C. elegans* zygote

III. Intracellular Turing pattern formation

Intracellular protein concentration gradients

- An important difference between intracellular gradients and multicellular morphogen gradients is that degradation does not play a significant role in the formation of intracellular gradients.
- This is a consequence of the fact that the lifetime of a typical protein exceeds the duration of the cellular process regulated by the presence of a gradient.
- Instead, some modification in the protein, such as its phosphorylation state, changes as it moves away from the catalytic source of the modification.

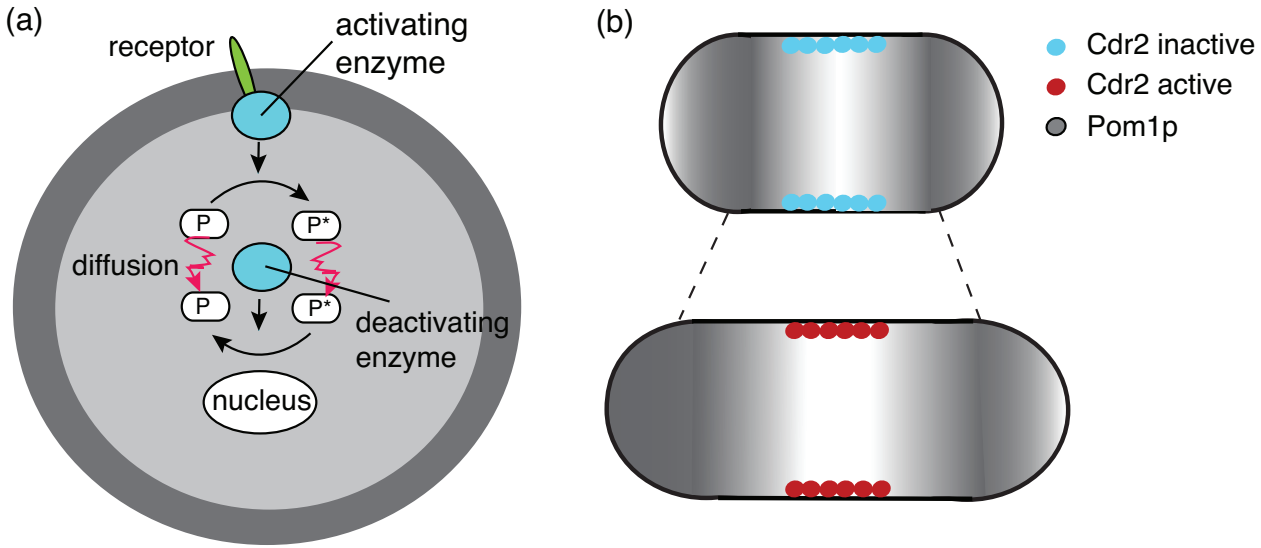

Protein gradients in C. elegans embryos[7]

- Intracellular protein gradients regulate cell division in C. elegans one-cell zygote
- Mex-5 and PIE-1 form opposing gradients
- Both proteins rapidly switch between fast and slow diffusing states with kinetics that vary along the anterior/posterior axis of the cell
- Kinetic polarization generated by PAR polarity system

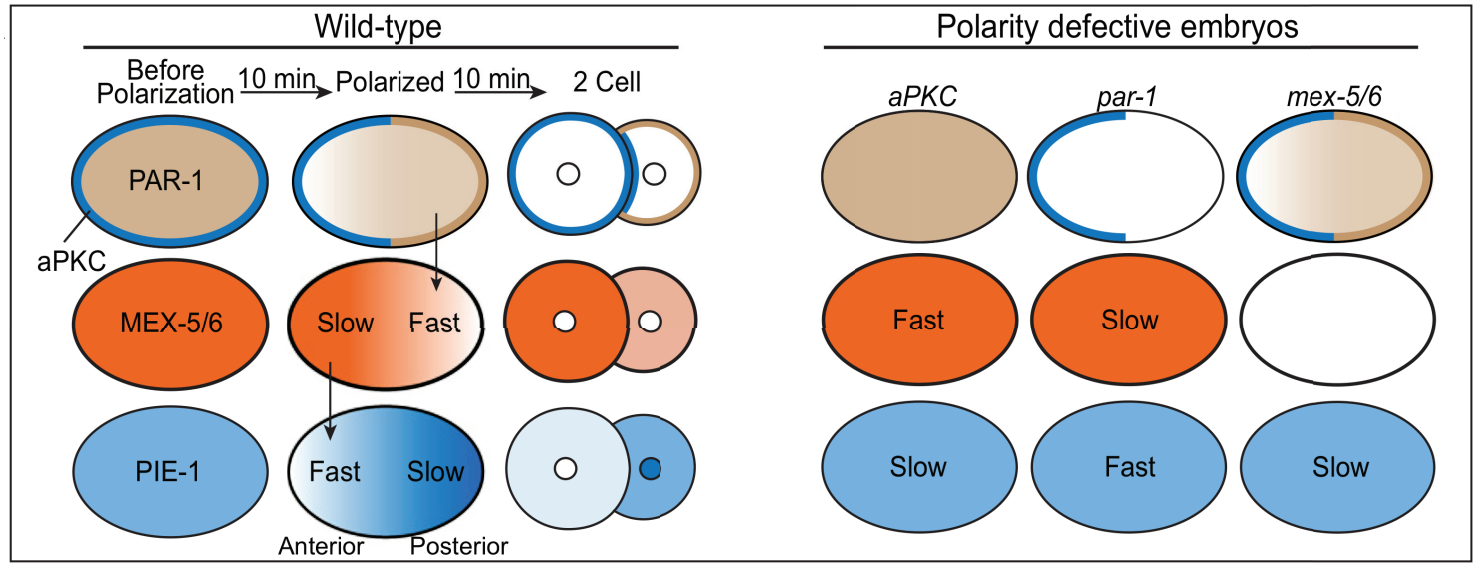

[7] Wu et al PNAS 2018

RAPID DIFFUSION STATE SWITCHING IN C. ELEGANS ZYGOTE

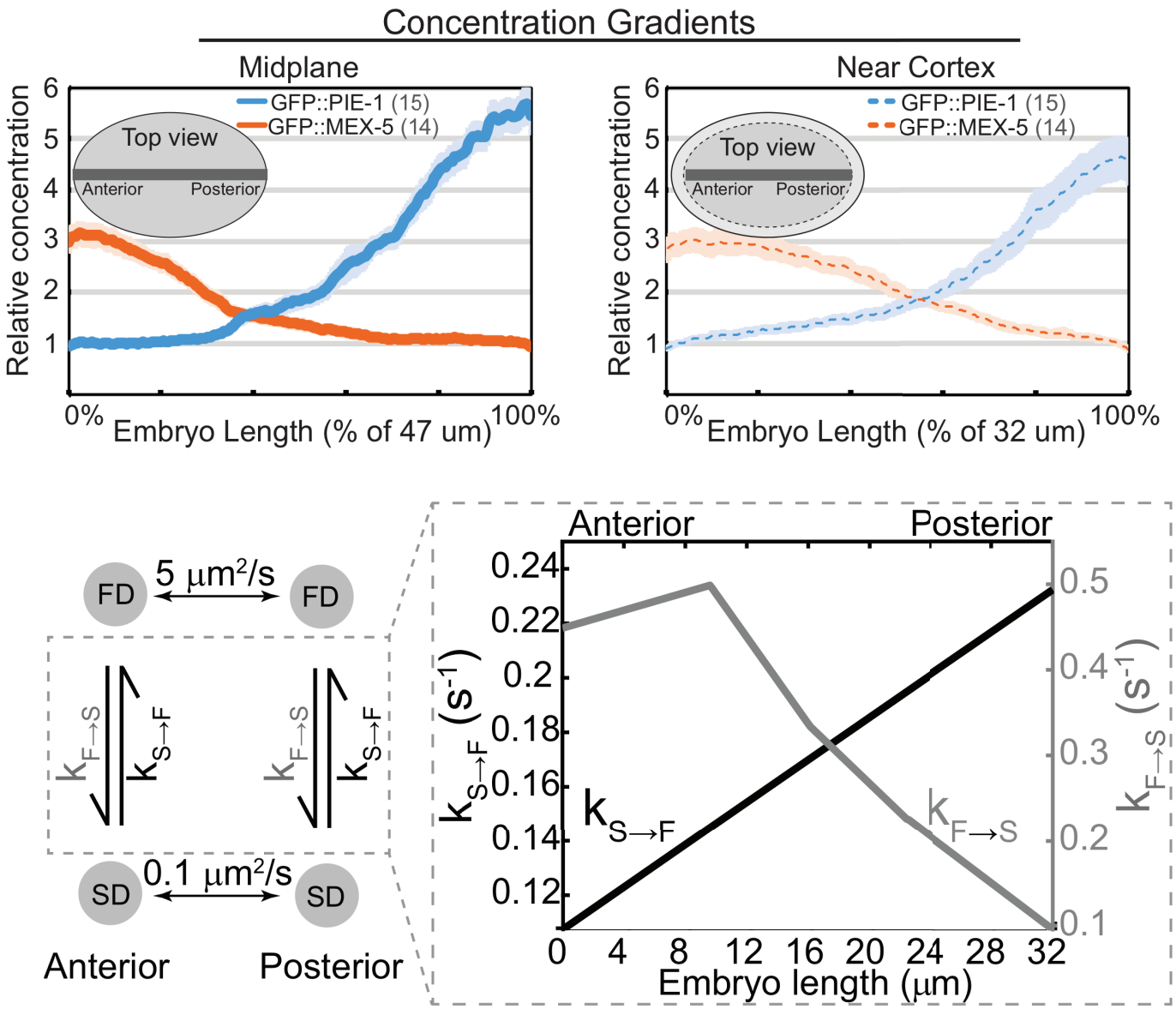

SPACE-DEPENDENT SWITCHING BROWNIAN MOTIONS[8]

- Suppose switching conformational states have different diffusivities $D_0 \underset{\alpha/\epsilon}{\overset{\beta/\epsilon}{\rightleftharpoons}} D_1$
- Consider the hybrid Wiener process

$$dX(t) \quad = \quad \sqrt{2D_{N(t)}}dW(t), \quad N(t) \in \{0,1\}$$

- Suppose that the switching rates α, β depend on the current position of the particle, $\alpha = \alpha(X(t))$, $\beta = \beta(X(t))$.

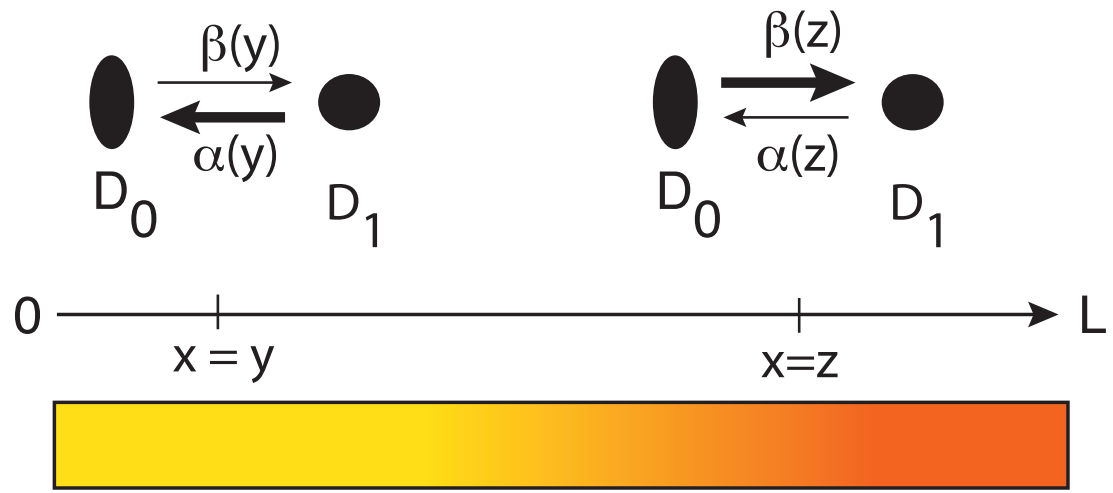

[8] PCB and Lawley Phys Rev E 2017, 2019

Reaction-diffusion equations

- At the population level we have the densities $C_n(x,t)$, $n = 0, 1$, evolve according to

$$\frac{\partial C_0}{\partial t} = D_0 \frac{\partial^2 C_0}{\partial x^2} - \beta(x) C_0 + \alpha(x) C_1$$
$$\frac{\partial C_1}{\partial t} = D_1 \frac{\partial^2 C_1}{\partial x^2} + \beta(x) C_0 - \alpha(x) C_1,$$

  with reflecting boundary conditions

$$\partial_x C_0(0,t) = \partial_x C_1(0,t) = 0,\ \partial_x C_0(L,t) = \partial_x C_1(L,t) = 0.$$

  and the initial conditions $C_n(x,0) = C_n^*$.

- Typical length of *C. elegans* is $L = 32\mu$m and switching rates are around $0.1\ \text{s}^{-1}$.
- Introducing the fundamental time-scale $\tau = L^2/D$ with $D \sim 1\mu m^2/s$ yields $\tau \sim 1000s$.
- Fast switching regime: rescale switching rates $\alpha, \beta \to \alpha/\epsilon, \beta/\epsilon$ with $\alpha, \beta = O(1)$

FAST SWITCHING LIMIT

- Decompose the density C_n as

$$C_n(x,t) = C(x,t)\rho_n(x) + \epsilon w_n(x,t),$$

where $\sum_n w_n(x,t) = 0$ and

$$\rho_0(x) = \frac{\alpha(x)}{\alpha(x)+\beta(x)}, \quad \rho_1(x) = 1 - \rho_0(x).$$

- Substituting this decomposition into RD equations and then adding the pair of equations gives

$$\frac{\partial C}{\partial t} = \frac{\partial^2 \overline{D}(x) C}{\partial x^2} + \epsilon \sum_{n=0,1} D_n \frac{\partial^2 w_n}{\partial x^2},$$

where

$$\overline{D}(x) = \sum_{n=0,1} D_n \rho_n(x).$$

BROWNIAN MOTION WITH ITO SPACE-DEPENDENT DIFFUSIVITY

- Taking $\lim_{\epsilon \to 0}$ yields the diffusion equation

$$\frac{\partial C}{\partial t} = \frac{\partial^2}{\partial x^2}(\overline{D}(x)C),$$

with no-flux boundary conditions $\partial_x \overline{D}(x)C(x,t) = 0$ at $x = 0, L$.

- At single particle level have the Ito SDE

$$dX(t) = \sqrt{2\overline{D}(X(t))}\, dW(t), \quad \overline{D}(x) = \sum_{n=0,1} \rho_n(x) D_n$$

- The steady-state solution takes the form

$$C^*(x) = \frac{A}{\overline{D}(x)}, \quad \int_0^L C^*(x)dx = L[C_0^* + C_1^*]$$

- Normalization condition implies that

$$A = L[C_0^* + C_1^*] \left[\int_0^L \frac{dx}{\overline{D}(x)} \right]^{-1}.$$

Reproduce results of Wu et al. 2018

- Approximate the switching rates for MEX-5 and PIE-1 using piecewise constant functions.

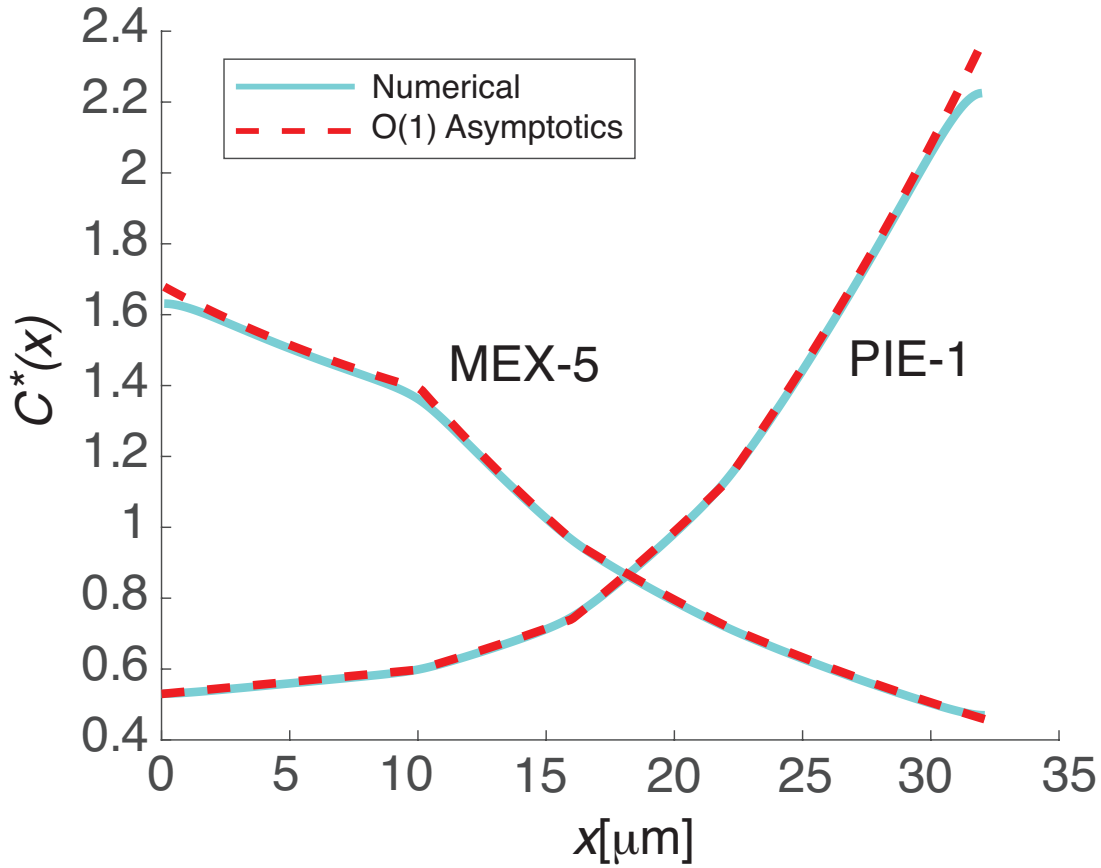

BOUNDARY LAYERS

- Original RD system involves two coupled diffusion equations so that at each boundary there are two boundary conditions: reflecting BCs for C_0 and C_1.
- On the other hand, the reduced diffusion equation for the scalar $C = C_0 + C_1$ has a single boundary condition at each end.
- Singular perturbation problem: solution to the scalar equation represents an outer solution that is valid in the bulk of the domain, but has to be matched to an inner solution at each boundary.

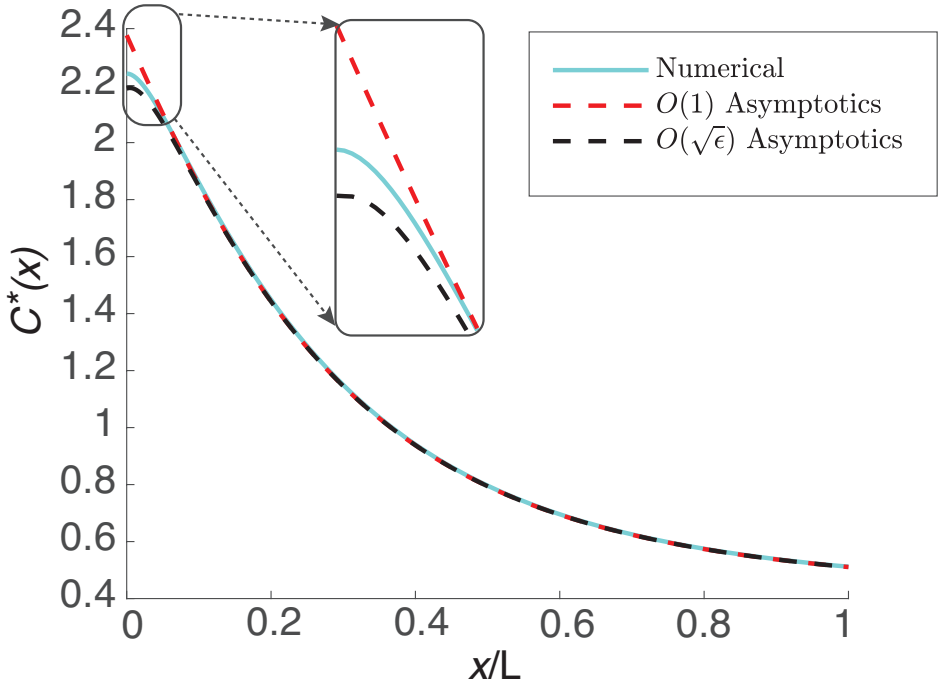

Outline of talk

I. Cytoneme-based morphogenesis

II. Switching diffusions and protein gradients in *C. elegans* zygote

III. Intracellular Turing pattern formation

Classical Turing mechanism[9]

- Two nonlinearly interacting chemical species differing significantly in their rates of diffusion can amplify spatially periodic fluctuations in their concentrations, resulting in the formation of a stable periodic pattern.

$$\frac{\partial u}{\partial t} = D_u \nabla^2 u + f(u,v), \qquad \frac{\partial v}{\partial t} = D_v \nabla^2 v + g(u,v).$$

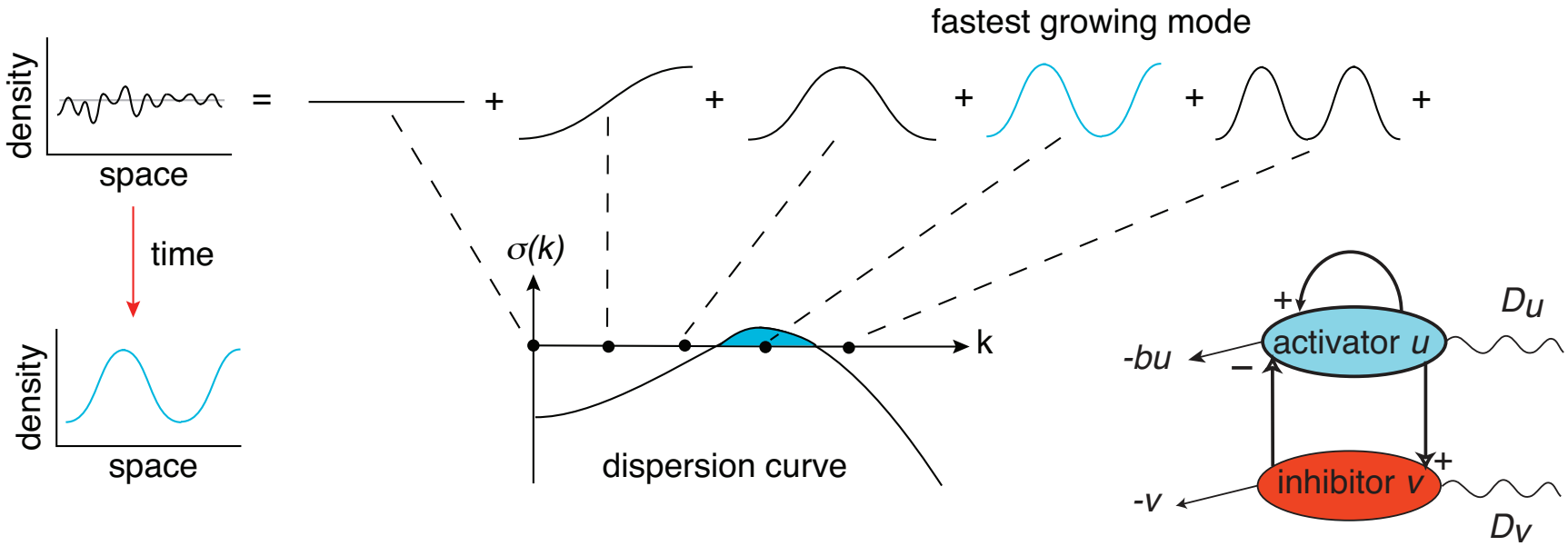

- Gierer and Meinhardt: one way to generate a Turing instability is an activator-inhibitor system: a slowly diffusing chemical activator and a quickly diffusing chemical inhibitor.

[9] Turing 1952

Intracellular Turing pattern formation

- Many examples of spatiotemporal patterns of signaling molecules at the intracellular level – regulate downstream structures that drive cell polarization and cell division (cytoskeleton, cell membrane)
- Classical Turing mechanism does not work at subcellular length and time scales.
- Many intracellular processes are mass-conserving
- Intracellular patterns typically involve the dynamical exchange of proteins between the cytoplasm and plasma membrane, resulting in associated changes of conformational state and a spatial redistribution of mass.

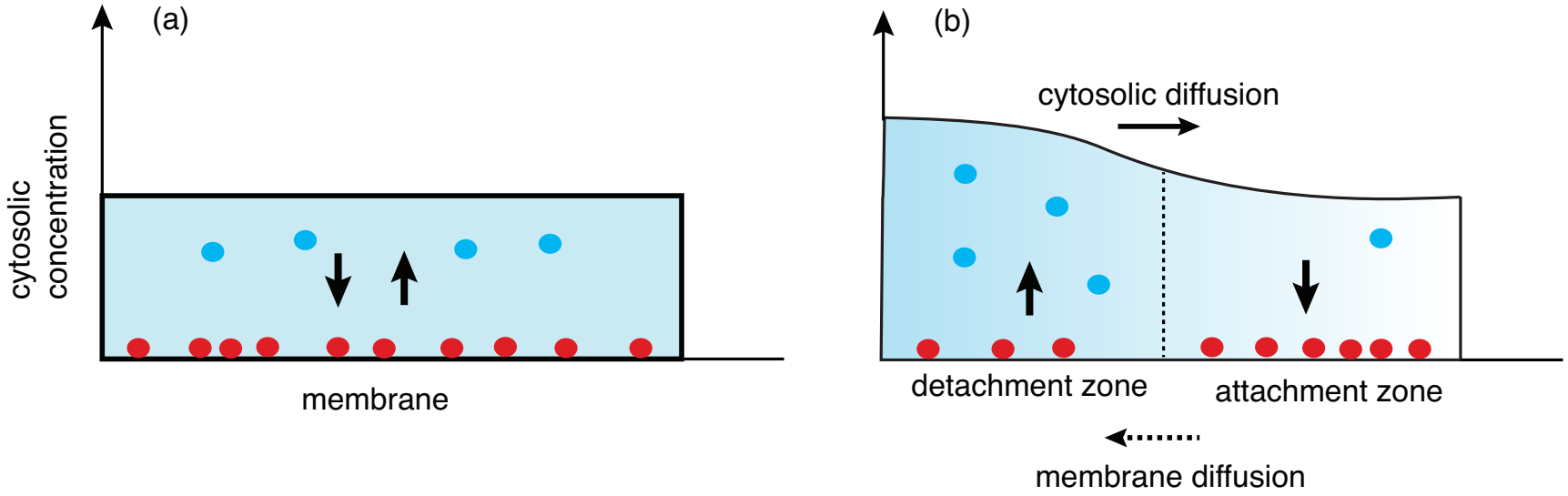

- Hybrid reaction transport models that couple diffusion and active motor-driven transport eg. synaptogeneisis in *C. elegans*

Mass conservation[10]

- Mass-conserving RD system

$$\frac{\partial u}{\partial t} = D_u \frac{\partial^2 u}{\partial x^2} + f(u,v), \quad \frac{\partial v}{\partial t} = D_v \frac{\partial^2 v}{\partial x^2} - f(u,v),$$

- Mass conservation condition

$$\bar{n} = \int_0^L n(x,t)dx, \quad n(x,t) = u(x,t) + v(x,t).$$

- Let (u^*, v^*) denote a fixed point of the system, which satisfies the pair of equations

$$f(u^*, v^*) = 0, \quad u^* + v^* = \bar{n} := \frac{N}{L}. \tag{0.1}$$

- Linearizing about (u^*, v^*) using uniform perturbations yields the following eigenpairs:

$$\sigma_1 = 0, \quad \mathbf{e}_1 = \begin{pmatrix} -f_v/f_u \\ 1 \end{pmatrix}; \quad \sigma_2 = f_u - f_v, \quad \mathbf{e}_2 = \begin{pmatrix} -1 \\ 1 \end{pmatrix}.$$

- Marginally stable to perturbations that change the mass density – eigenvector tangential to the reactive nullcline $f(u,v) = 0$. The second eigenpair determines the local stability of fixed points against mass-conserving perturbations.

[10] Ishihara et al 2007, Halatek and Frey 2018

MASS CONSERVATION

- Suppose that $f_u < f_v$. Inclusion of diffusion can induce a spatially periodic redistribution of the mass density, resulting in corresponding displacements of the local equilibria.

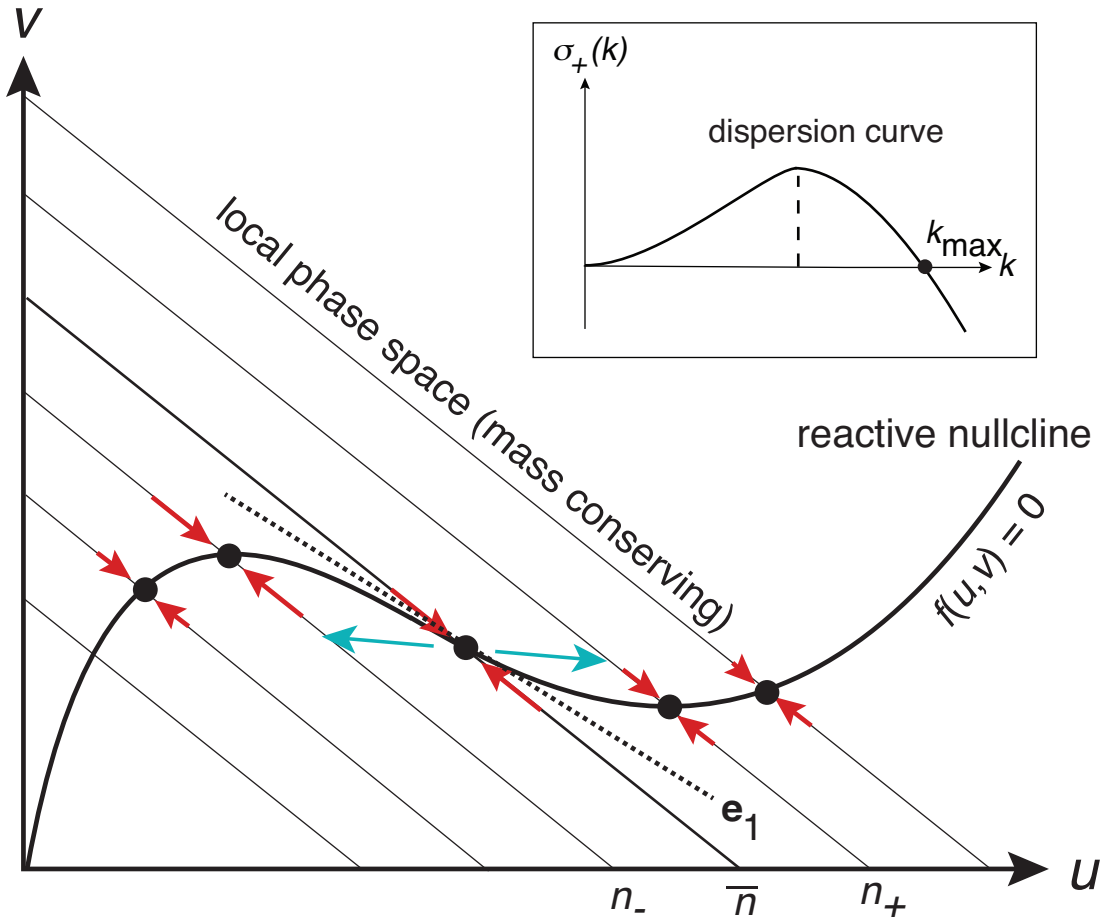

Cell polarization in fission yeast

- Fission yeast is a rod-shaped cell consisting of two hemispheres of constant radius that cap a cylinder of increasing length.
- Immediately following cell division, the cell initially grows at one end only, namely, the "old end" of the previous cell cycle (monopolar growth).
- Later in the cell cycle, the cell also starts growing from the new end (bipolar growth), in a process known as "new end take off" (NETO) Cell growth then ceases during cell division.

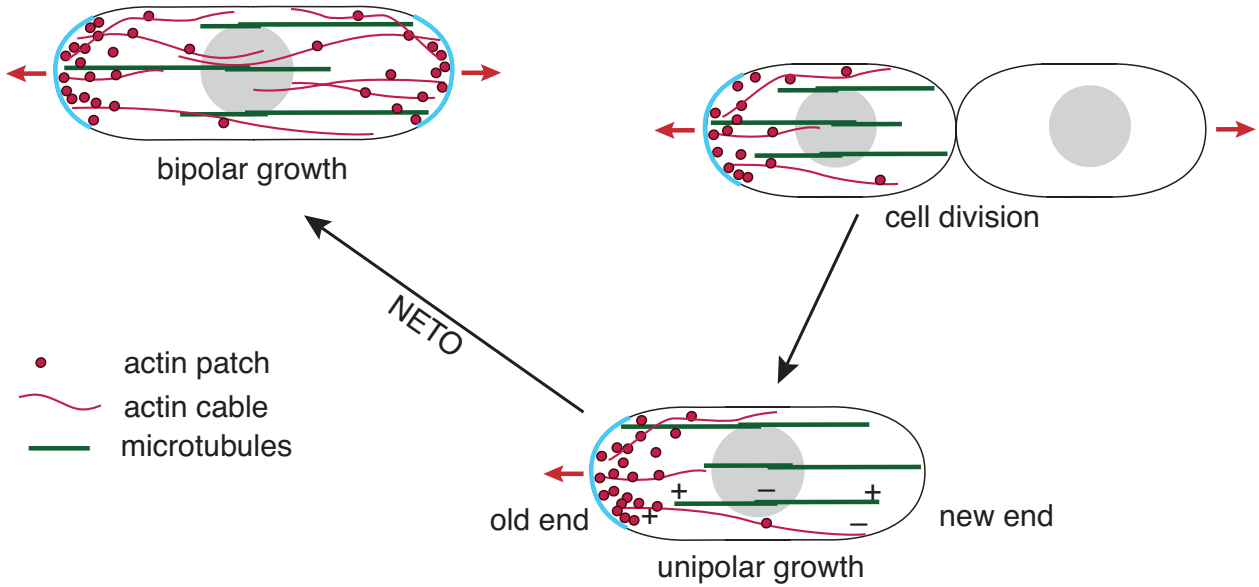

- The Rho GTPase Cdc42 plays an important role in regulating polarized growth in fission yeast. NETO is correlated with a switch from asymmetric to symmetric out-of-phase Cdc42 oscillations at the poles of the cell

PDE-ODE model of Cdc42 oscillations in fission yeast[11]

- Let $C(x,t)$ be the cytosolic concentration of Cdc42 at x and $X_i(t)$, $i = 1, 2$, the concentration of Cdc42 at the i-th compartment, where $t, t > 0$, denotes time.The PDE-ODE model is taken to be

$$\frac{\partial C(x,t)}{\partial t} = D\frac{\partial^2 C(x,t)}{\partial x^2}, \quad 0 < x < L, \quad t > 0,$$

with flux boundary conditions

$$-D\partial_x C(0,t) = -f(X_1(t), C(0,t)), \quad -D\partial_x C(L,t) = f(X_2(t), C(L,t))$$

$$\frac{dX_1}{dt} = f(X_1(t), C(0,t)), \quad \frac{dX_2}{dt} = f(X_2(t), C(L,t))$$

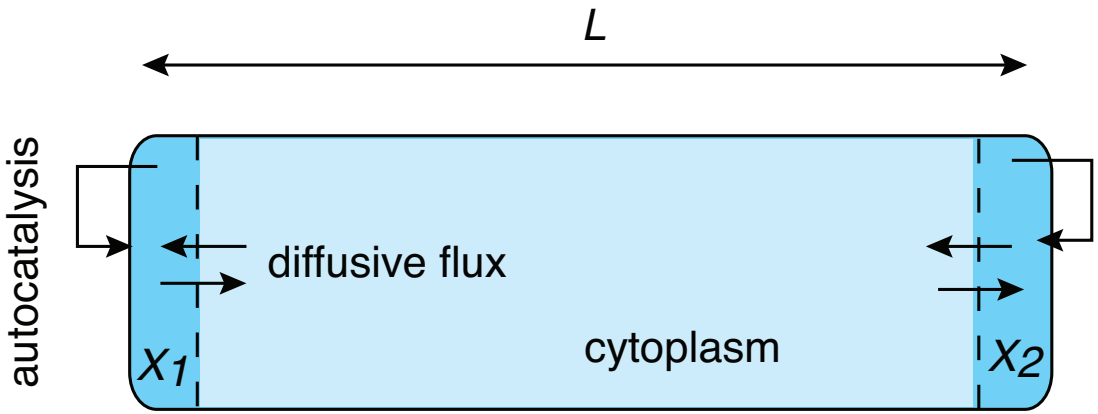

[11] PCB and Xu 2018

HOMEOSTATIC CONTROL OF SYNAPTIC DENSITY IN *C elegans*

During larval development of *C. elegans*, the density of ventral and dorsal cord synapses containing the glutamate receptor GLR-1 is maintained despite significant changes in neurite length[12].

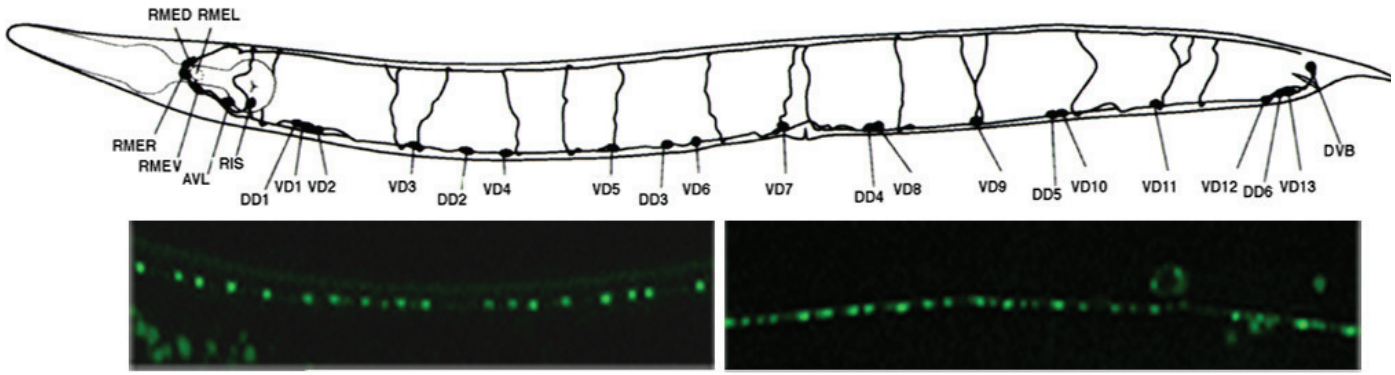

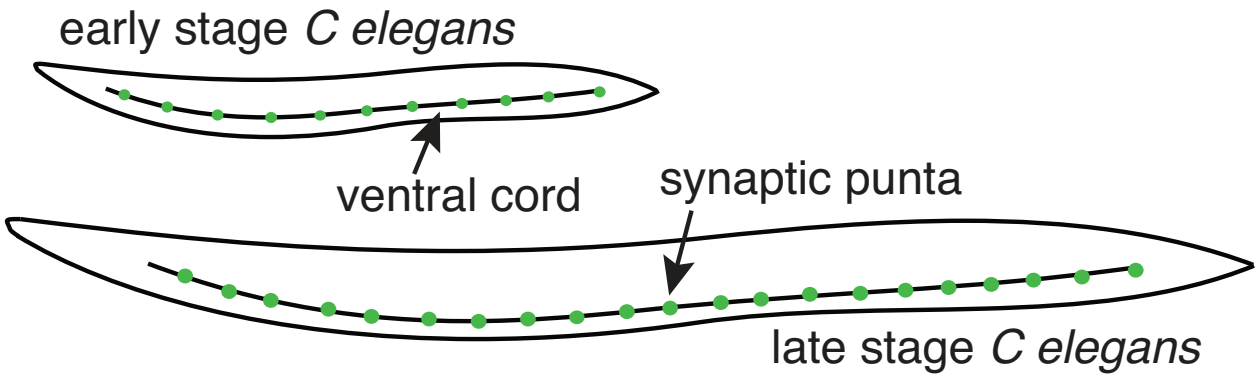

[12] Rongo et al 1999

(a) Calcium influx through voltage-gated calcium channels activates CaMKII, which enhances the active transport and delivery of GLR-1 to synapses [13].

(b) Under conditions of increased excitation, higher calcium levels results in constitutively active CaMKII failing to localize at synapses, leading to the removal of GLR-1 from synapses

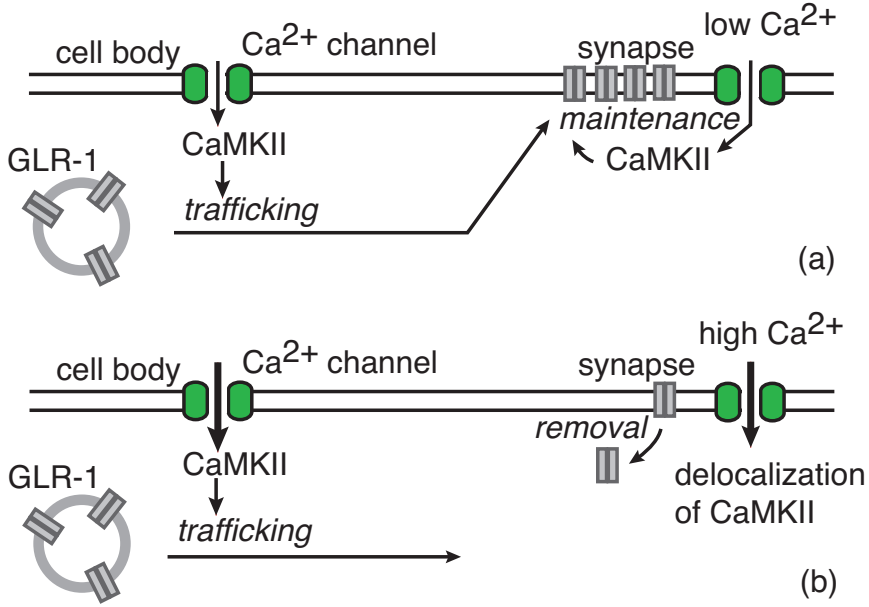

How do interactions between diffusing CaMKII molecules and GLR-1 establish and maintain synaptic density during growth?

[13] Maricq et al Neuron 2013, 2015

HYBRID TRANSPORT MODEL[14]

- Hypothesis I: the formation of a regularly spaced distribution of synaptic puncta at an early stage of development is due to a spontaneous pattern forming mechanism
- Hypothesis II: Nonlinear interactions between a slowly diffusing species (CaMKII) with concentration U and a rapidly advecting species (GLR-1) switching between anterograde (R_+) and retrograde (R_-) motor-driven transport.

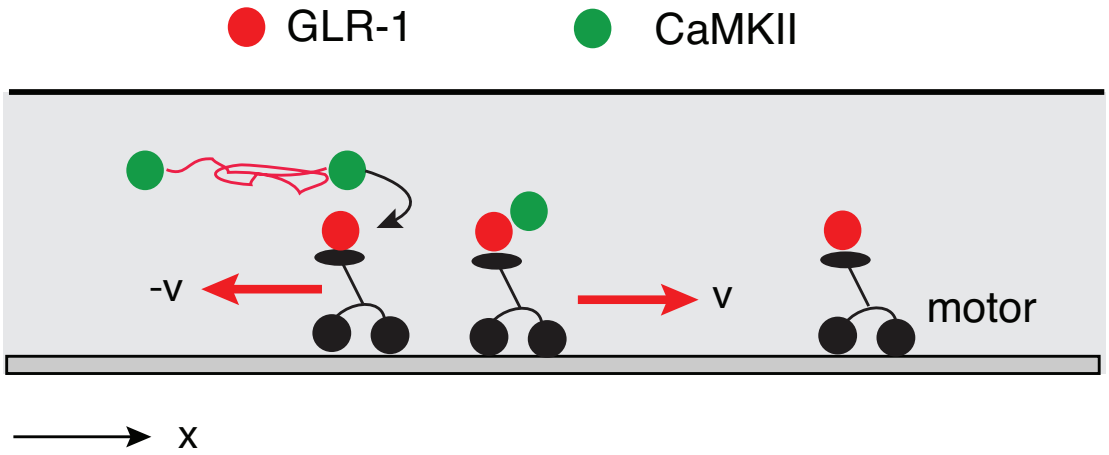

[14] PCB and Heather Brooks SIADS 2016, Phys. Rev. E 2017

$$\frac{\partial U}{\partial t} = D\frac{\partial^2 U}{\partial x^2} + f(R_+ + R_-, U), \quad \left.\frac{\partial U(x,t)}{\partial x}\right|_{x=0,L} = 0$$

$$\frac{\partial R_+}{\partial t} = -v\frac{\partial R_+}{\partial x} + \alpha R_- - \beta R_+ + g(R_+, U), \; vR_+(0,t) = vR_-(0,t)$$

$$\frac{\partial R_-}{\partial t} = v\frac{\partial R_-}{\partial x} + \beta R_+ - \alpha R_- + g(R_-, U), \; vR_+(L,t) = vR_-(L,t)$$

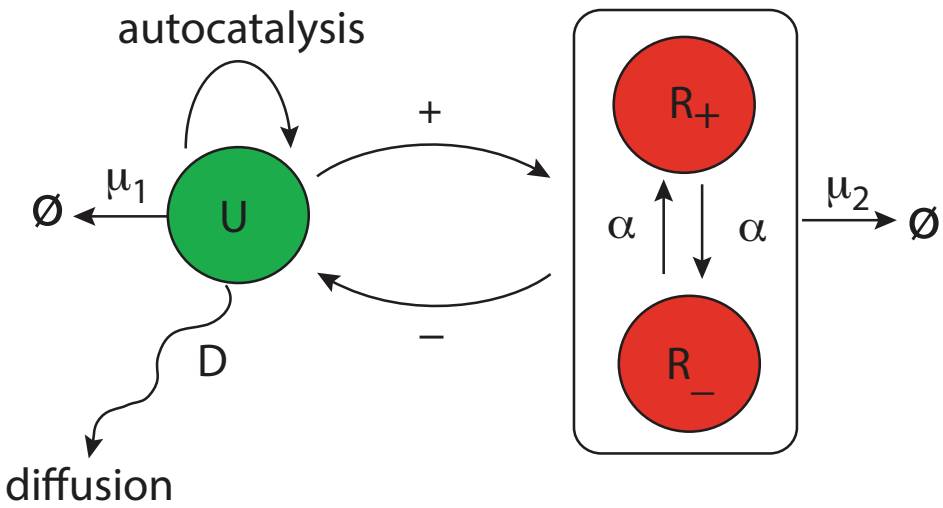

- Choose the classical activator-inhibitor system of Gierer and Meinhardt

$$f(R,U) = \rho_1 \frac{U^2}{R} - \mu_1 U$$
$$g(R,U) = \rho_2 U^2 - \mu_2 R.$$

ρ_1, ρ_2 are strength of interactions, μ_1 and μ_2 are decay rates.

- Hypothesis III: the maintenance of synaptic density as the organism grows is due to "pulse or stripe insertion" of a spatially periodic pattern on a growing domain.

STEADY-STATE SOLUTIONS

- Steady-state equations are equivalent to classical GM model.
- Introduce the flux $J = v(R_+ - R_-)$ and total concentration $R = R_+ + R_-$.

$$
\begin{aligned}
0 &= D\frac{d^2U}{dx^2} + \rho_1\frac{U^2}{R} - \mu_1 U,\\
0 &= -v\frac{dR_+}{dx} + \alpha R_- - \beta R_+ + \rho_2 U^2 - \mu_2 R_+,\\
0 &= v\frac{dR_-}{dx} + \beta R_+ - \alpha R_- + \rho_2 U^2 - \mu_2 R_-.
\end{aligned}
$$

$$
\begin{aligned}
0 &= D\frac{d^2U}{dx^2} + \rho_1\frac{U^2}{R} - \mu_1 U,\\
0 &= -\frac{dJ}{dx} + \rho_2 U^2 - \mu_2 R,\\
0 &= -v^2\frac{dR}{dx} - (2\alpha + \mu_2)J.
\end{aligned}
$$

- Use third equation on RHS to eliminate J:

$$
\begin{aligned}
0 &= D\frac{d^2U}{dx^2} + \rho_1\frac{U^2}{R} - \mu_1 U,\\
0 &= \widehat{D}\frac{d^2R}{dx^2} + \rho_2 U^2 - \mu_2 R, \quad \widehat{D} = \frac{v^2}{2\alpha + \mu_2}
\end{aligned}
$$

- However, linear stability analysis of full model differs from reduced model

PUNCTA INSERTION ON A SLOWLY GROWING DOMAIN

- Numerical simulations showing temporal evolution of $U, R_{\pm}$ on a slowly growing domain. Length changes from $10\mu m$ to $100\mu m$ in 2 hours.
- Insertion of new peaks maintains synaptic density (2-3 per 10 μm).

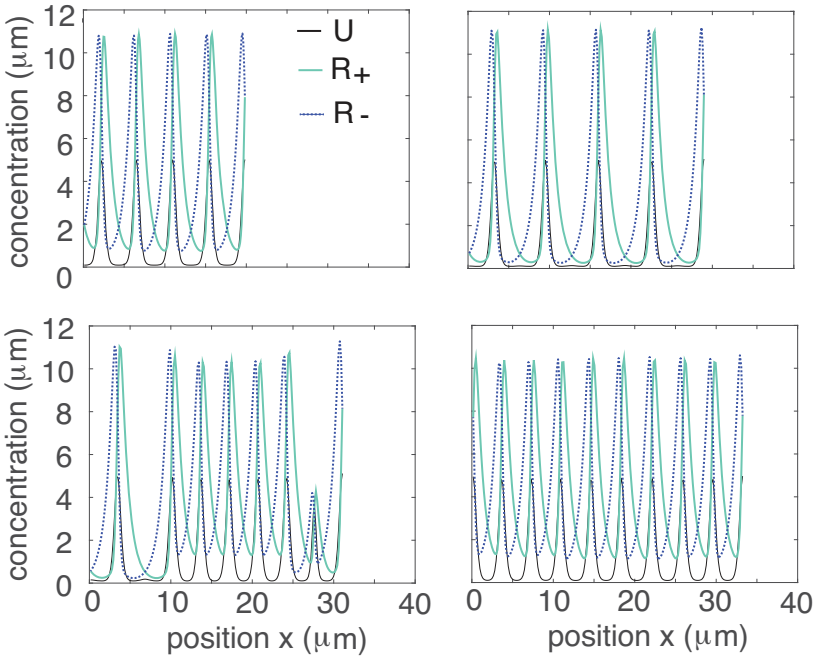

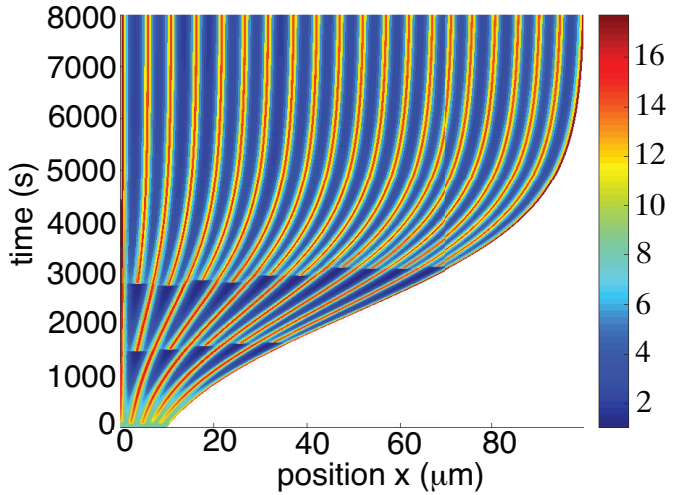

Prediction: Pattern depends on the diffusivity of CaMKII, the speed and switching rates of molecular motors, and the rate of CaMKII phosphorylation. Manipulation of these parameters should change the synaptic spacing, but the insertion of new puncta should persist.